

Electronic Supplementary Information for

Synthesis and characterisation of ruthenium-nitrosyl complexes in oxygen-rich ligand environments.

V. Mahesh Krishnan, Hadi D. Arman, and Zachary J. Tonzetich*

Department of Chemistry, University of Texas at San Antonio, San Antonio, TX 78249
zachary.tonzetich@utsa.edu

Contents	Pages
Figure S1. Infrared spectrum of 1 as a thin film.	S2
Figure S2. Infrared spectrum of 2 as a thin film.	S2
Figure S3. Infrared spectrum of 3 as a thin film.	S3
Figure S4. Infrared spectrum of 4 as a thin film.	S3
Figure S5. Electronic absorption spectrum of 1 in dichloromethane.	S4
Figure S6. Electronic absorption spectrum of 2 in dichloromethane.	S4
Figure S7. Electronic absorption spectrum of 3 in dichloromethane.	S5
Figure S8. Electronic absorption spectrum of 4 in dichloromethane.	S5
Figure S9. Infrared spectrum of 2+ as a thin film.	S6
Figure S10. Electronic absorption spectrum of 2+ in dichloromethane.	S6
Figure S11. ^1H NMR spectrum of 2+ in acetonitrile- d_3 .	S7
Figure S12. Electronic absorption spectrum of 5+ in dichloromethane.	S7
Figure S13. ^1H NMR spectrum of 5+ in chloroform- d .	S7
Figure S14. Electronic absorption spectrum of 5+ in dichloromethane.	S8
Figure S15. ^1H NMR spectrum of 6 in chloroform- d .	S8
Figure S16. Cyclic voltammograms of 1 in dichloromethane.	S9
Figure S17. Cyclic voltammograms of 2 in dichloromethane.	S9
Figure S18. Cyclic voltammogram of 4 in dichloromethane.	S10
Figure S19. Cyclic voltammograms of 5+ in dichloromethane.	S10
Figure S20. Thermal ellipsoid drawing of 1 .	S11
Figure S21. Thermal ellipsoid drawing of 3 .	S12
Figure S22. Thermal ellipsoid drawing of 4 .	S13
Table S1. Crystallographic data and refinement parameters for 1-3 .	S14
Table S2. Crystallographic data and refinement parameters for 4 and 7 .	S15

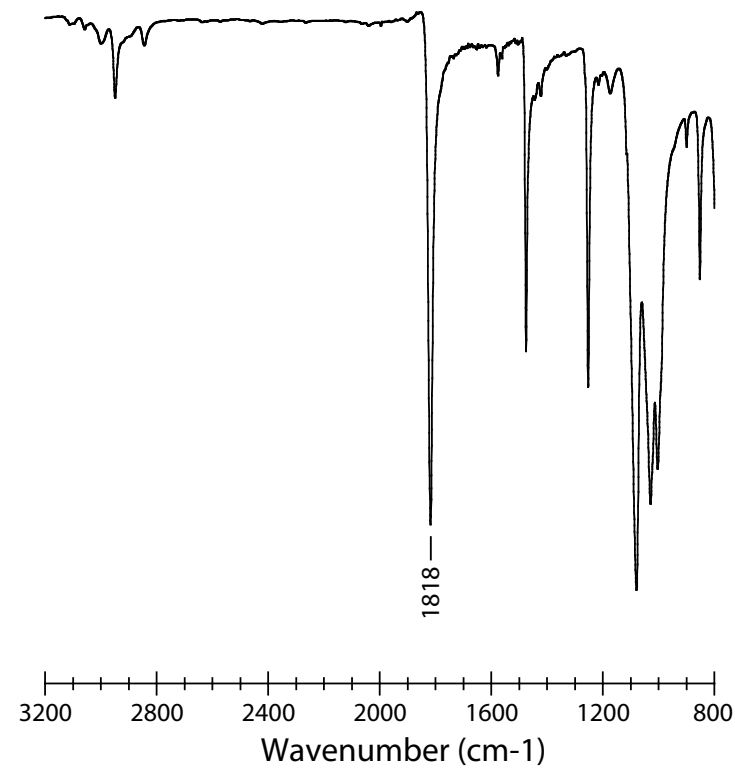


Figure S1. Infrared spectrum of $[\text{Ru}(\text{L}_{\text{OMe}})(\text{NO})(\text{H}_4\text{Cat})]$ (**1**) as a thin film on NaCl.

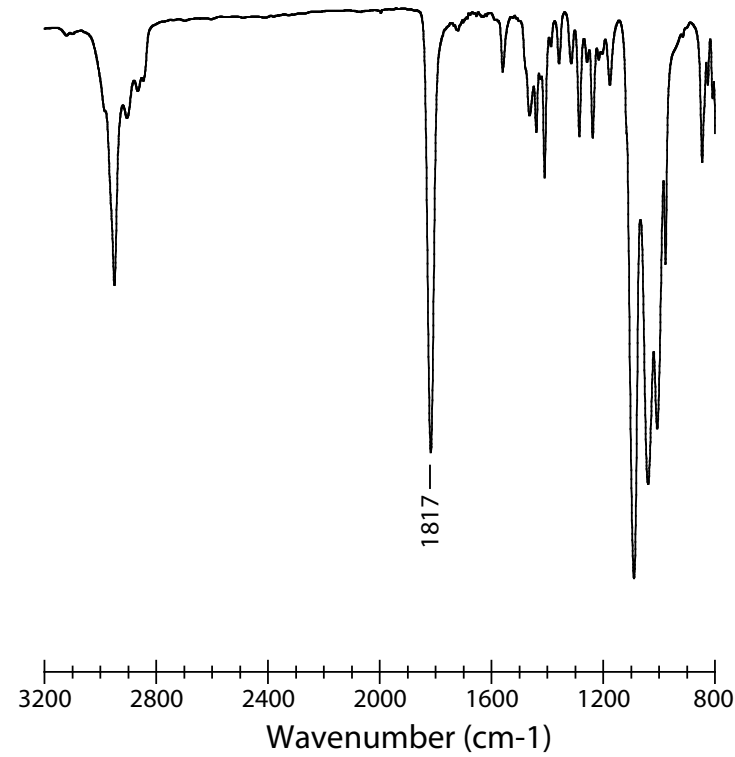


Figure S2. Infrared spectrum of $[\text{Ru}(\text{L}_{\text{OMe}})(\text{NO})(\text{Bu}_2\text{Cat})]$ (**2**) as a thin film on NaCl.

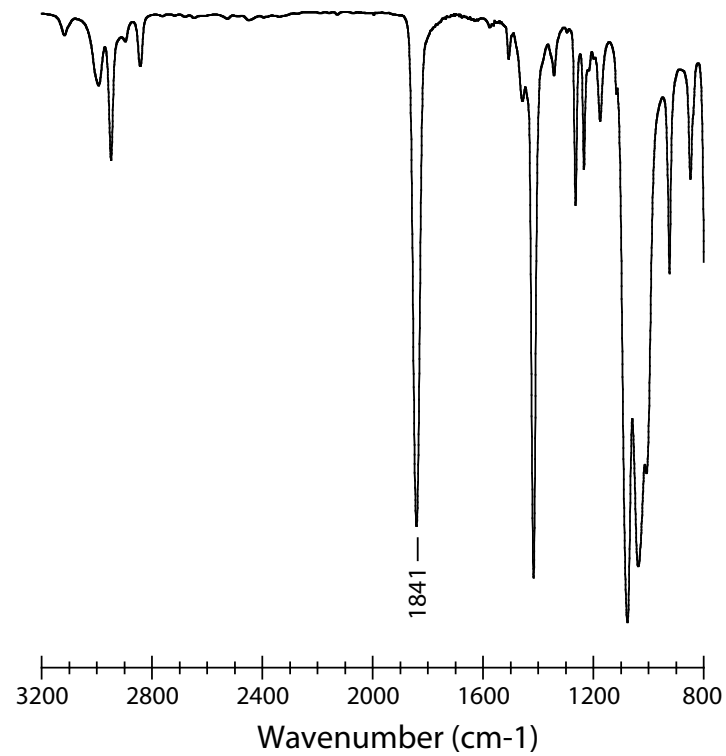


Figure S3. Infrared spectrum of $[\text{Ru}(\text{L}_{\text{OMe}})(\text{NO})(\text{Br}_4\text{Cat})]$ (**3**) as a thin film on NaCl.

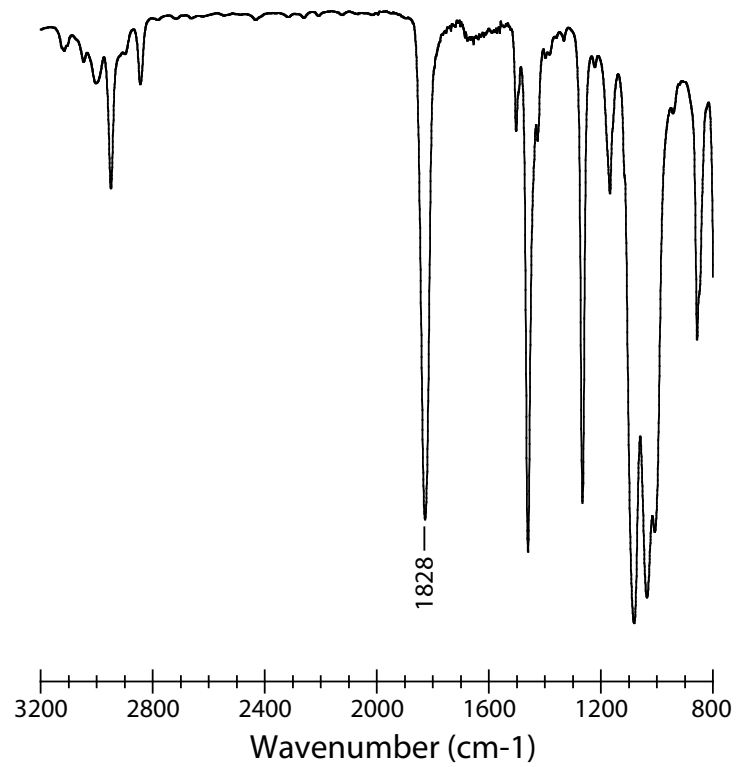


Figure S4. Infrared spectrum of $[\text{Ru}(\text{L}_{\text{OMe}})(\text{NO})(\text{NaphCat})]$ (**4**) as a thin film on NaCl.

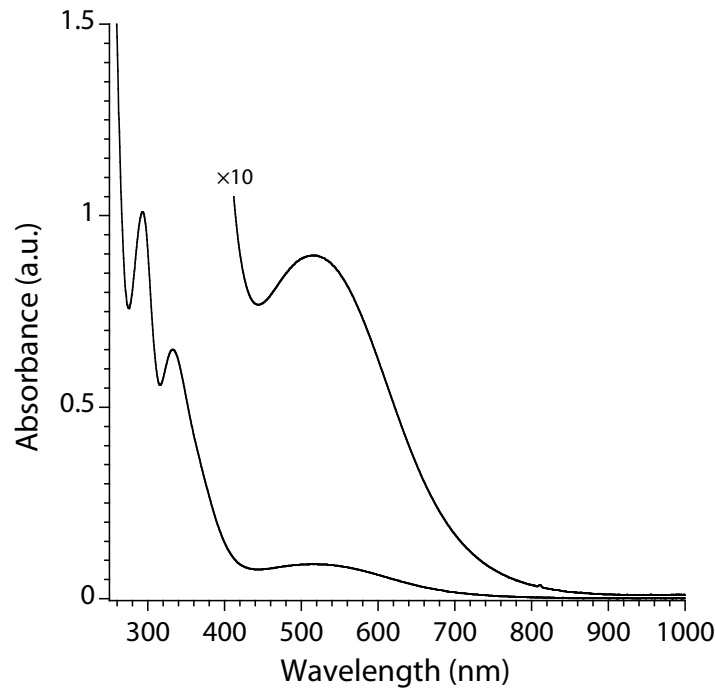


Figure S5. Electronic absorption spectrum of $[\text{Ru}(\text{L}_{\text{OMe}})(\text{NO})(\text{H}_4\text{Cat})]$ (**1**) in dichloromethane.

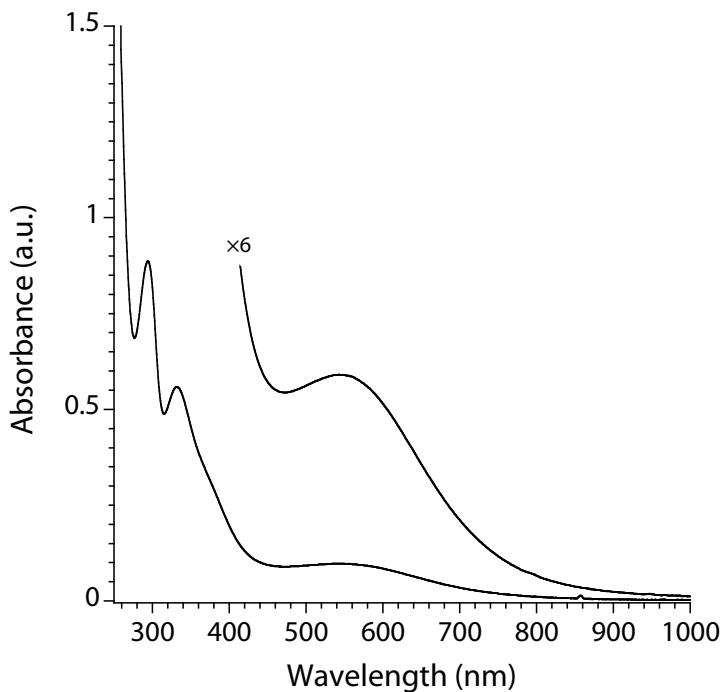


Figure S6. Electronic absorption spectrum of $[\text{Ru}(\text{L}_{\text{OMe}})(\text{NO})(\text{'Bu}_2\text{Cat})]$ (**2**) in dichloromethane.

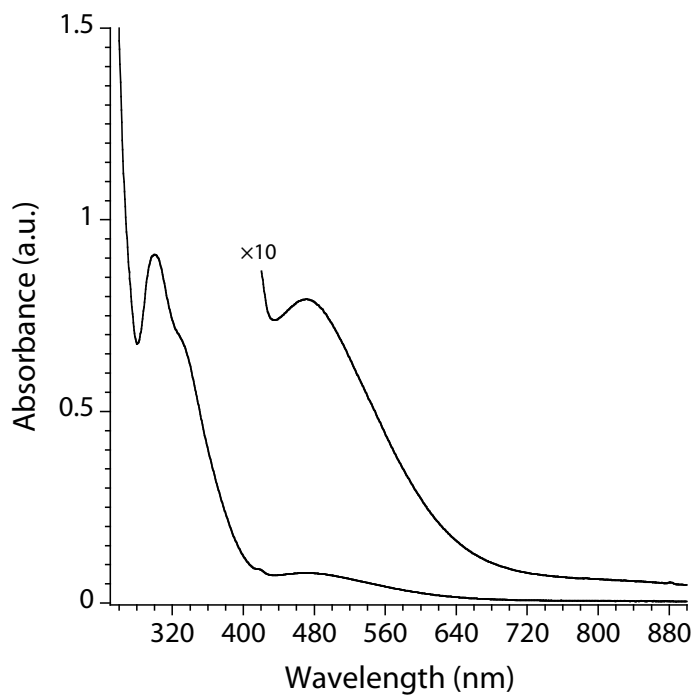


Figure S7. Electronic absorption spectrum of $[\text{Ru}(\text{L}_{\text{OMe}})(\text{NO})(\text{Br}_4\text{Cat})]$ (**3**) in dichloromethane.

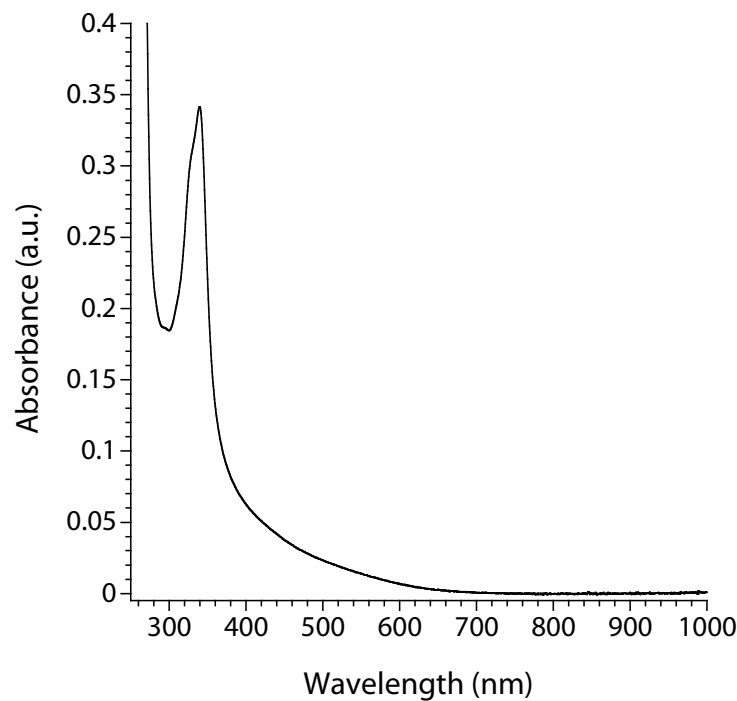


Figure S8. Electronic absorption spectrum of $[\text{Ru}(\text{L}_{\text{OMe}})(\text{NO})(\text{NaphCat})]$ (**4**) in dichloromethane.

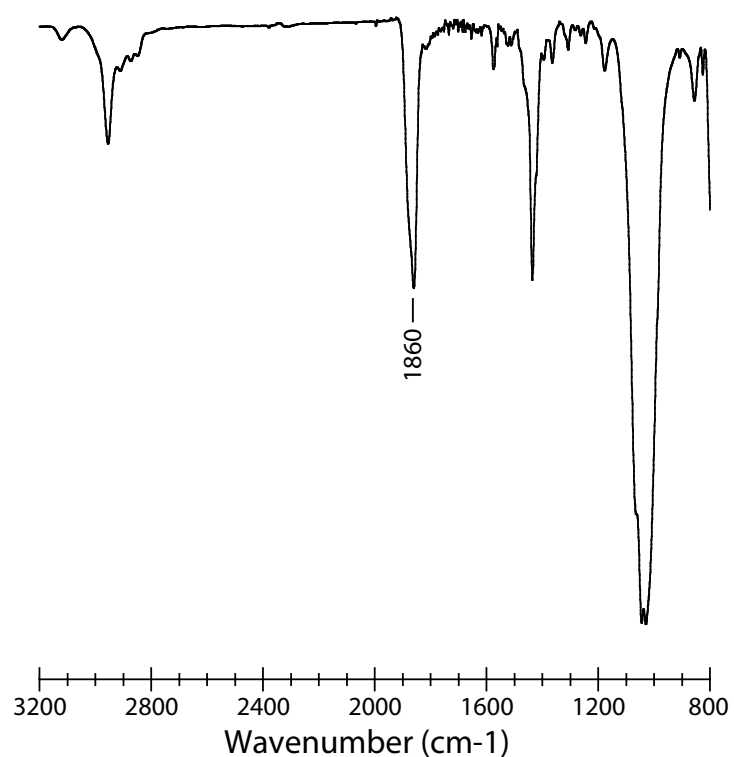


Figure S9. Infrared spectrum of $[\text{Ru}(\text{L}_{\text{OMe}})(\text{NO})(\text{Bu}_2\text{cat})](\text{BF}_4)$ ($\mathbf{2}^+$) as a thin film on NaCl.

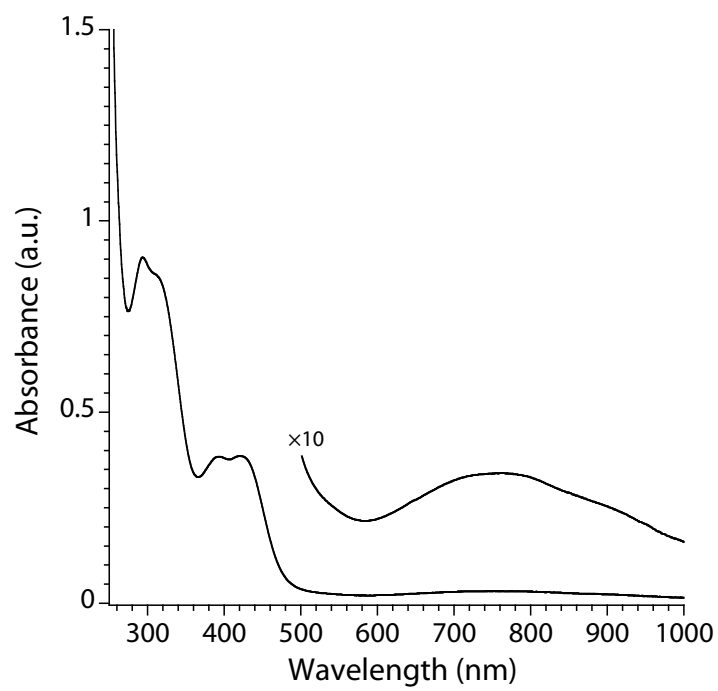


Figure S10. Electronic absorption spectrum of $[\text{Ru}(\text{L}_{\text{OMe}})(\text{NO})(\text{Bu}_2\text{cat})](\text{BF}_4)$ ($\mathbf{2}^+$) in dichloromethane.

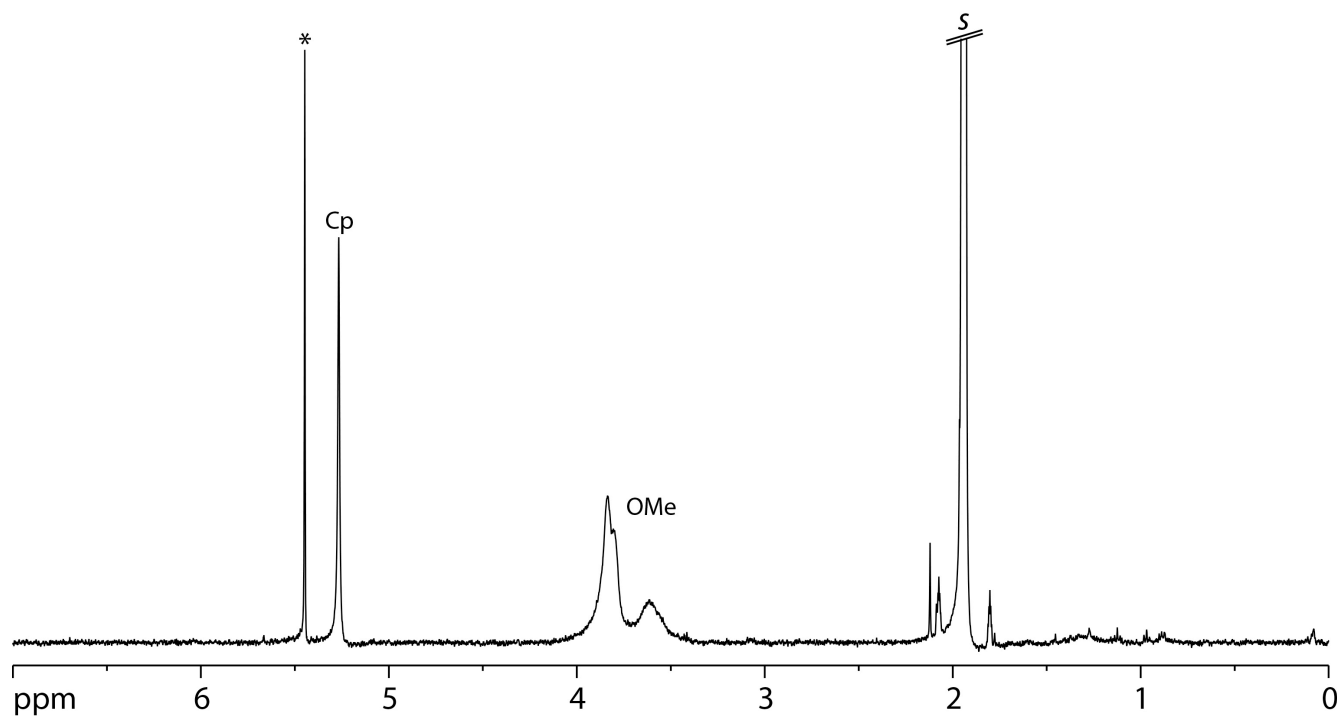


Figure S11. 500 MHz ^1H NMR spectrum of crude $[\text{Ru}(\text{L}_{\text{OMe}})(\text{NO})(\text{'Bu}_2\text{cat})](\text{BF}_4)$ ($\mathbf{2}^+$) in acetonitrile- d_3 (s). Asterisk denotes resonance due to residual dichloromethane.

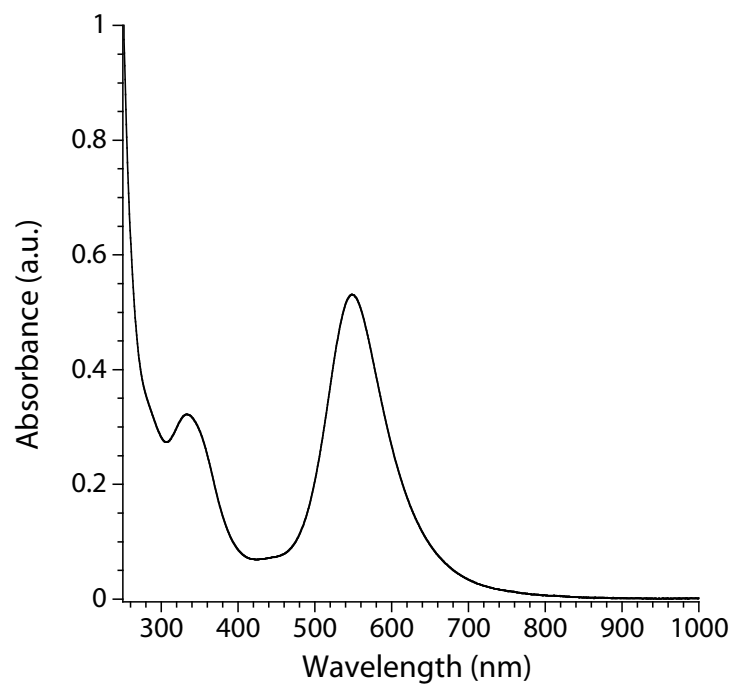


Figure S12. Electronic absorption spectrum of $[\text{Ru}(\text{L}_{\text{OMe}})(\text{NCCH}_3)(\text{'Bu}_2\text{quin})](\text{BF}_4)$ ($\mathbf{5}^+$) in dichloromethane obtained by photolysis of $\mathbf{2}^+$ in acetonitrile.

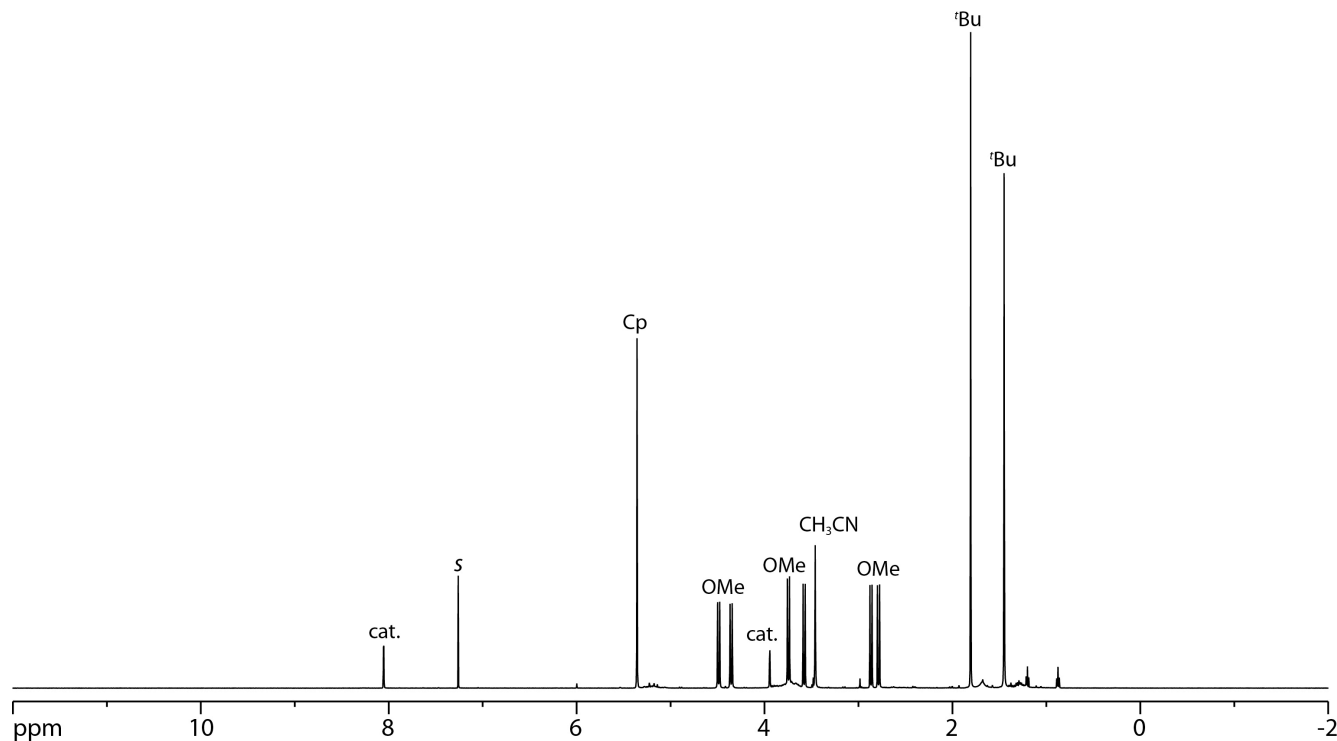


Figure S13. 500 MHz ^1H NMR spectrum (CDCl_3) of $[\text{Ru}(\text{L}_{\text{OMe}})(\text{NCCH}_3)(\text{'Bu}_2\text{quin})](\text{BF}_4)^-(\mathbf{5}^-)$ obtained by photolysis of $\mathbf{2}^+$ in acetonitrile.

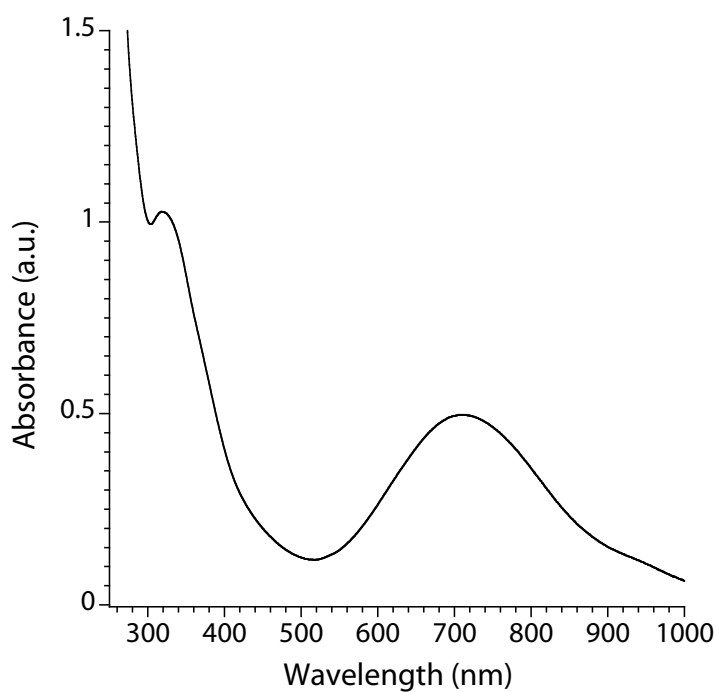


Figure S14. Electronic absorption spectrum of $[\text{Ru}(\text{L}_{\text{OMe}})(\text{NCCH}_3)(\text{Br}_4\text{cat})](\mathbf{6})$ in dichloromethane.

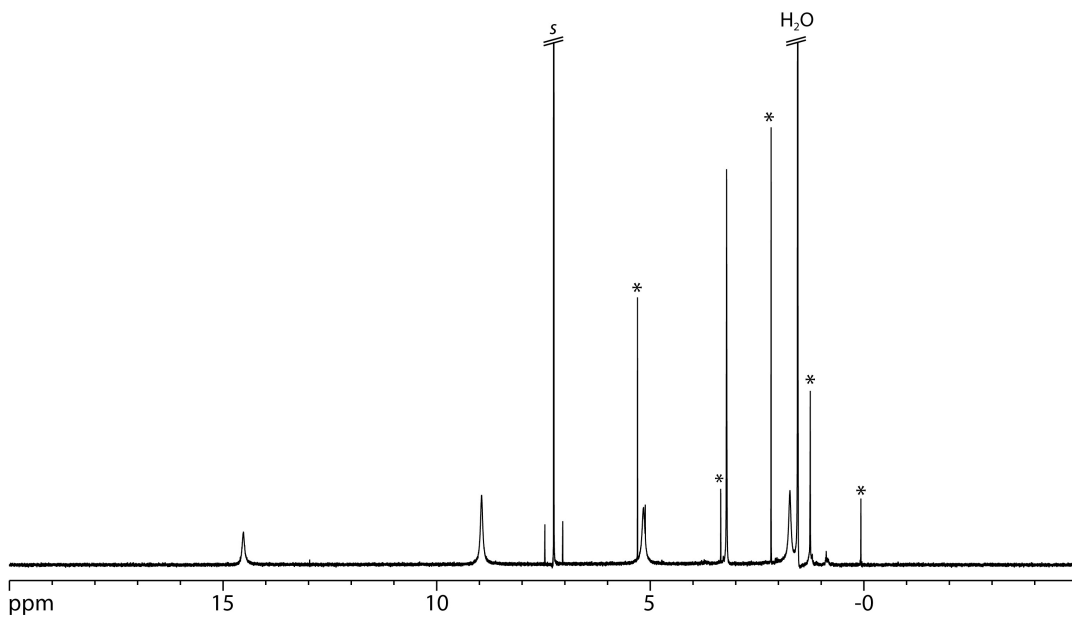


Figure S15. 500 MHz ^1H NMR spectrum (CDCl_3) of $[\text{Ru}(\text{L}_{\text{OMe}})(\text{NCCH}_3)(\text{Br}_4\text{cat})]$ (**6**) obtained by photolysis of **3** in a mixture of dichloroethane and acetonitrile. Asterisks denote resonances due to residual dichloromethane, dichloroethane, acetone and grease.

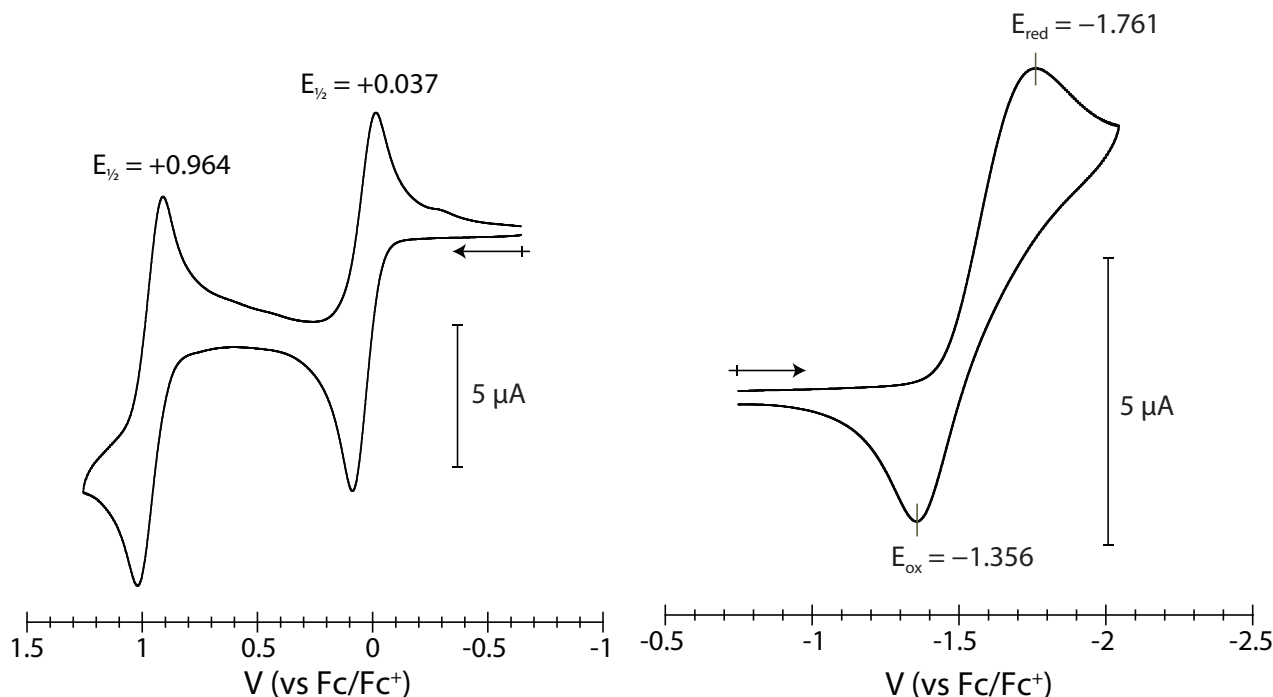


Figure S16. Anodic (left) and cathodic (right) portions of the cyclic voltammogram of $[\text{Ru}(\text{L}_{\text{OMe}})(\text{NO})(\text{H}_4\text{cat})]$ (**1**) at a Pt electrode in dichloromethane. The scan rate is 50 mV/s and the supporting electrolyte is 0.1 M Bu_4NPF_6 .

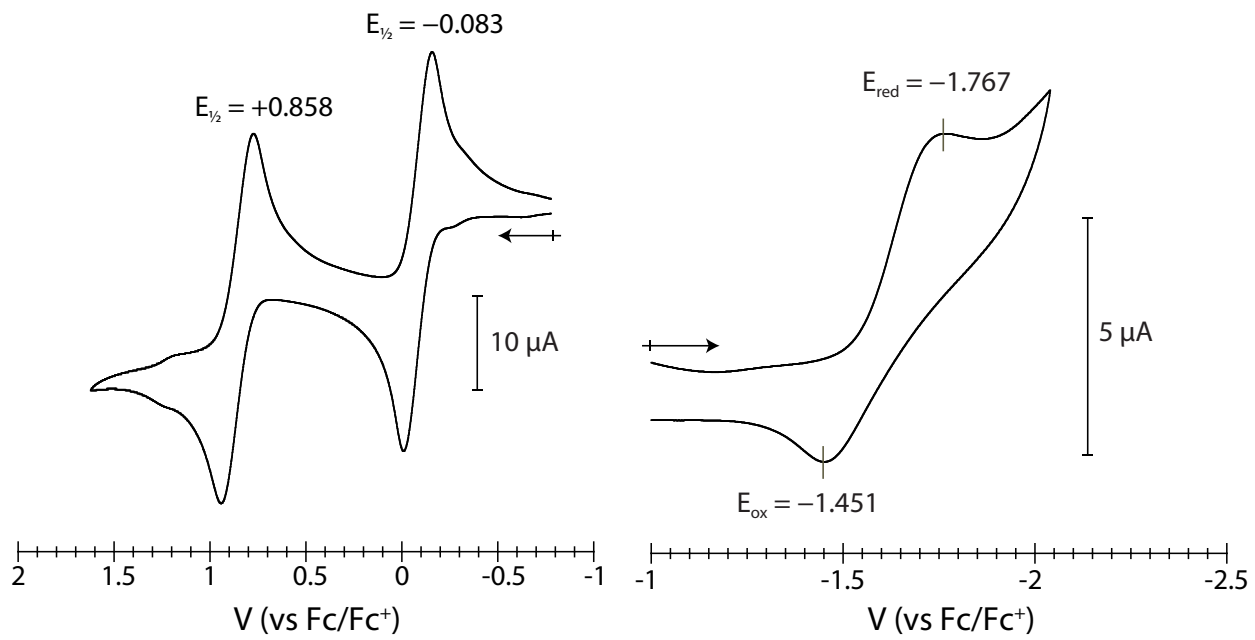


Figure S17. Anodic (left) and cathodic (right) portions of the cyclic voltammogram of $[\text{Ru}(\text{L}_{\text{OMe}})(\text{NO})(\text{'Bu}_2\text{cat})]$ (**2**) at a Pt electrode in dichloromethane. The scan rate is 50 mV/s and the supporting electrolyte is 0.1 M Bu_4NPF_6 .

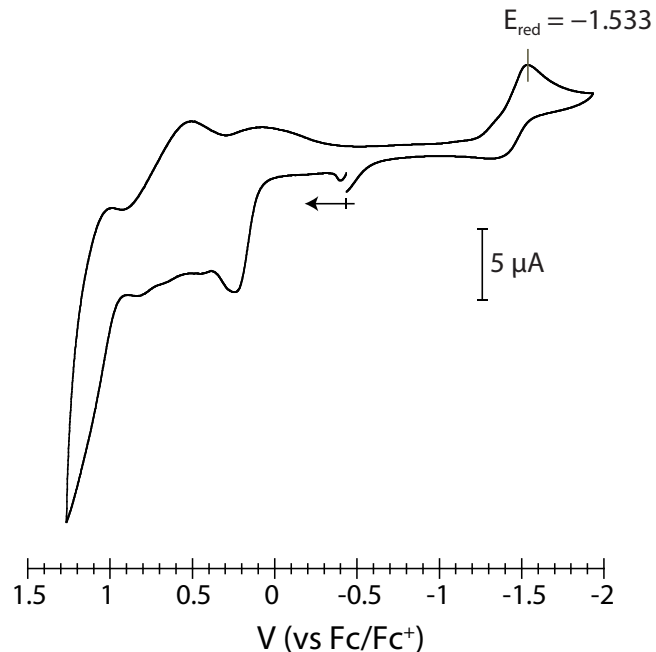


Figure S18. Cyclic voltammogram of $[\text{Ru}(\text{L}_{\text{OMe}})(\text{NO})(\text{Naphcat})]$ (**4**) at a Pt electrode in dichloromethane. The scan rate is 50 mV/s and the supporting electrolyte is 0.1 M Bu_4NPF_6 .

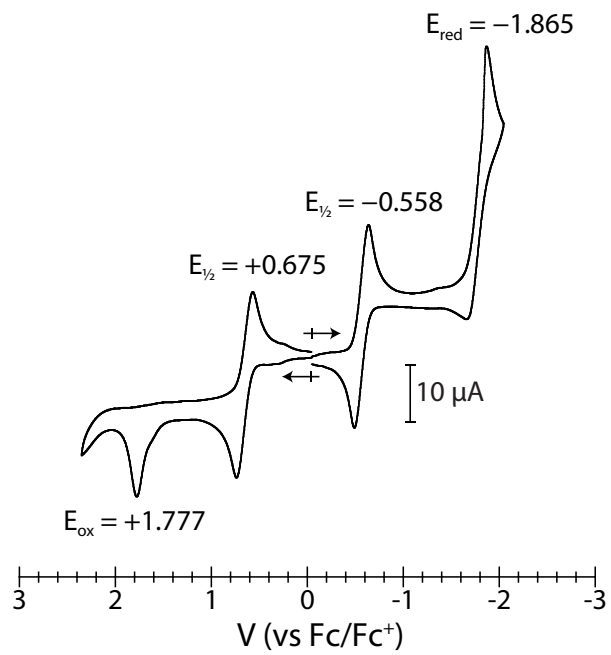


Figure S19. Cyclic voltammograms of $[\text{Ru}(\text{L}_{\text{OMe}})(\text{CH}_3\text{CN})(\text{'Bu}_2\text{quin})](\text{BF}_4)$ (**5+**) at a Pt electrode in dichloromethane. The scan rate is 50 mV/s and the supporting electrolyte is 0.1 M Bu_4NPF_6 .

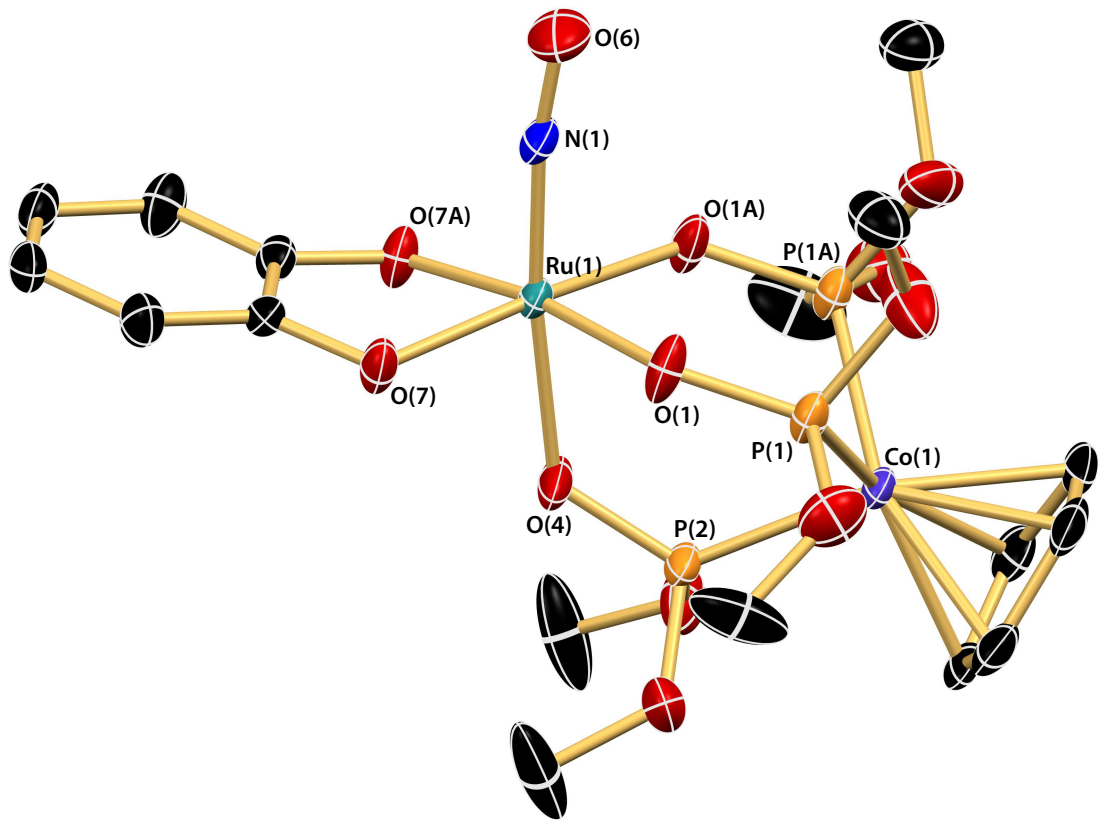


Figure S20. Thermal ellipsoid rendering (50%) of $[\text{Ru}(\text{L}_{\text{OMe}})(\text{NO})(\text{H}_4\text{cat})]$ (**1**). Hydrogen atoms omitted for clarity. Selected bond distances (\AA) and angles (deg): $\text{Ru}(1)\text{-N}(1) = 1.720(5)$; $\text{Ru}(1)\text{-O}(7) = 1.986(3)$; $\text{Ru}(1)\text{-O}(\text{avg}) = 2.062(4)$; $\text{N}(1)\text{-O}(12) = 1.166(7)$; $\text{Ru}(1)\text{-N}(1)\text{-O}(12) = 171.4(4)$.

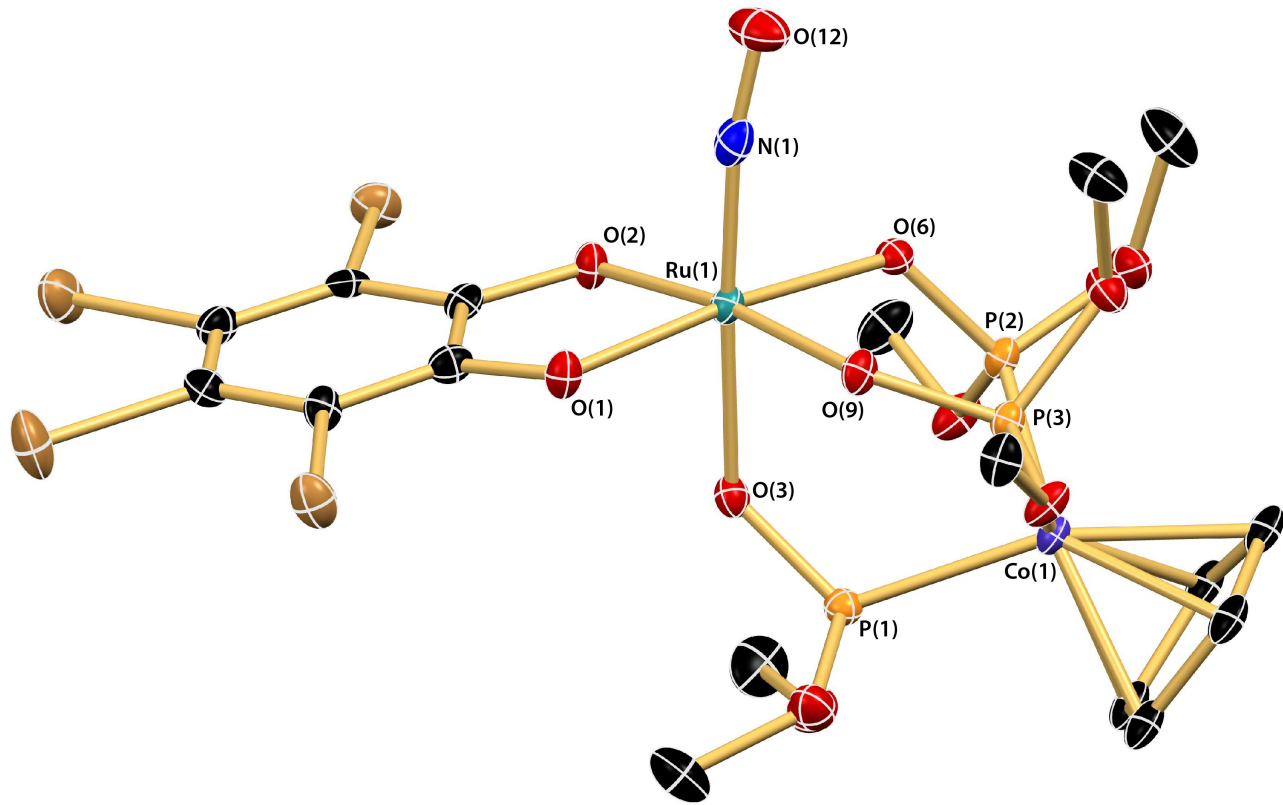


Figure S21. Thermal ellipsoid rendering (50%) of one of the two crystallographically independent molecules of $[\text{Ru}(\text{L}_{\text{OMe}})(\text{NO})(\text{Br}_4\text{cat})]$ (**3**) in the asymmetric unit. Hydrogen atoms omitted for clarity. Selected bond distances (\AA) and angles (deg): $\text{Ru}(1)\text{-N}(1) = 1.721(6)$; $\text{Ru}(1)\text{-O}(1) = 2.018(4)$; $\text{Ru}(1)\text{-O}(2) = 2.012(4)$; $\text{Ru}(1)\text{-O}(\text{avg}) = 2.073(4)$; $\text{N}(1)\text{-O}(12) = 1.188(7)$; $\text{Ru}(1)\text{-N}(1)\text{-O}(12) = 170.2(5)$.

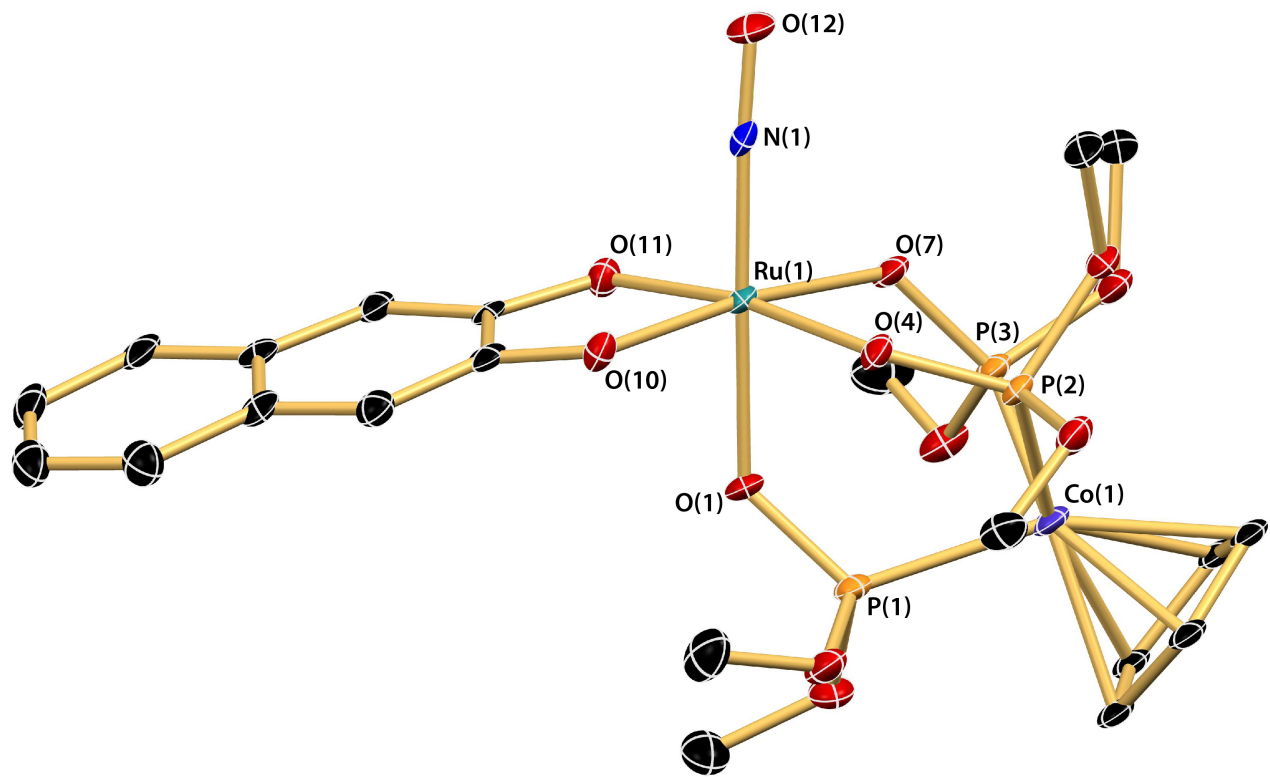


Figure S22. Thermal ellipsoid rendering (50%) of $[\text{Ru}(\text{L}_{\text{OMe}})(\text{NO})(\text{Naphcat})]$ (**4**). Hydrogen atoms omitted for clarity. Selected bond distances (\AA) and angles (deg): $\text{Ru}(1)\text{-N}(1) = 1.720(3)$; $\text{Ru}(1)\text{-O}(10) = 1.980(3)$; $\text{Ru}(1)\text{-O}(11) = 1.982(3)$; $\text{Ru}(1)\text{-O}(\text{avg}) = 2.063(3)$; $\text{N}(1)\text{-O}(12) = 1.162(4)$; $\text{Ru}(1)\text{-N}(1)\text{-O}(12) = 176.2(3)$.

Table S1. Crystallographic data and refinement parameters for compounds **1**-**3**.[‡]

Compound	1	2	3[§]
Empirical formula	C ₁₇ H ₂₇ NCoO ₁₂ P ₃ Ru	C ₂₅ H ₄₃ NCoO ₁₂ P ₃ Ru	C ₁₇ H ₂₃ NBr ₄ CoO ₁₂ P ₃ Ru
Formula weight (g/mol)	690.31	802.54	1005.91
Temperature (K)	98(2)	98(2)	98(2)
Crystal system, space group	Orthorhombic <i>Pnma</i>	Orthorhombic <i>Pbca</i>	Orthorhombic <i>Pca2</i> ₁
Unit cell dimensions (Å, deg)	<i>a</i> = 16.740(3) <i>b</i> = 11.664(2) <i>c</i> = 12.351(2)	<i>a</i> = 16.170(3) <i>b</i> = 17.167(3) <i>c</i> = 24.094(4)	<i>a</i> = 24.071(3) <i>b</i> = 14.2382(17) <i>c</i> = 17.677(2)
Volume (Å ³)	2411.6(7)	6688(2)	6058.5(13)
Z	4	8	8
Calculated density (g/cm ³)	1.901	1.594	2.206
Absorption coefficient (mm ⁻¹)	1.576	1.149	6.536
F(000)	1392	3296	3872
Crystal size (mm)	0.16 × 0.06 × 0.02	0.33 × 0.30 × 0.10	0.30 × 0.23 × 0.13
Θ range	2.40 to 27.50°	3.03 to 25.50°	2.98 to 27.43°
Limiting indices	-21 ≤ <i>h</i> ≤ 21, -15 ≤ <i>k</i> ≤ 11, -16 ≤ <i>l</i> ≤ 16	-19 ≤ <i>h</i> ≤ 19, -20 ≤ <i>k</i> ≤ 20, -29 ≤ <i>l</i> ≤ 27	-30 ≤ <i>h</i> ≤ 30, -18 ≤ <i>k</i> ≤ 18, -22 ≤ <i>l</i> ≤ 21
Reflections collected / unique	17093 / 2896 [R _{int} = 0.0628]	42240 / 6203 [R _{int} = 0.0661]	45644 / 12832 [R _{int} = 0.0485]
Completeness to Θ	99.9%	99.7%	99.8%
Absorption correction	multi-scan ABSCOR	multi-scan ABSCOR	multi-scan ABSCOR
Min. and max transmission	0.749 and 1.000	0.449 and 1.000	0.594 and 1.000
Data / restraints / parameters	2896 / 0 / 169	6203 / 0 / 400	12832 / 1 / 692
Goodness-of-fit on F ²	1.013	1.047	1.060
Final R indices [I > 2σ(I)]	R ₁ = 0.0454, wR ₂ = 0.1228	R ₁ = 0.0432, wR ₂ = 0.1091	R ₁ = 0.0308, wR ₂ = 0.0557
R indices (all data)	R ₁ = 0.0493, wR ₂ = 0.1264	R ₁ = 0.0497, wR ₂ = 0.1138	R ₁ = 0.0397, wR ₂ = 0.0577
Largest diff. peak and hole (e·Å ⁻³)	2.124 and -0.795	1.210 and -1.053	0.552 and -0.583

[‡]Refinement method was full-matrix least-squares on F²; wavelength = 0.71073 Å. R₁ = $\sum |F_o - F_c| / \sum |F_o|$; wR₂ = $\{ \sum [w(F_o^2 - F_c^2)^2] / \sum [w(F_o^2)^2] \}^{1/2}$. [§]Compound **3** was refined as an inversion twin.

Table S2. Crystallographic data and refinement parameters for compounds **4** and **7**.[‡]

Compound	4	7
Empirical formula	C ₂₁ H ₂₉ NCoO ₁₂ P ₃ Ru	C ₂₂ H ₄₄ N ₃ CoF ₆ O ₁₈ P ₃ RuS ₂
Formula weight (g/mol)	690.31	802.54
Temperature (K)	98(2)	298(2)
Crystal system, space group	Monoclinic <i>P</i> 2 ₁ /c	Monoclinic <i>C</i> c
Unit cell dimensions (Å, deg)	<i>a</i> = 10.4496(16) <i>b</i> = 11.5244(17) <i>c</i> = 22.855(4) β = 97.413(3)	<i>a</i> = 20.084(3) <i>b</i> = 12.6011(17) <i>c</i> = 16.863(2) β = 93.902(2)
Volume (Å ³)	2729.3(7)	4257.8(10)
Z	4	4
Calculated density (g/cm ³)	1.802	1.669
Absorption coefficient (mm ⁻¹)	1.399	1.050
F(000)	1496	2172
Crystal size (mm)	0.18 × 0.17 × 0.10	0.50 × 0.44 × 0.30
Θ range	1.965 to 25.500°	3.453 to 25.049°
Limiting indices	-12 ≤ <i>h</i> ≤ 7, -13 ≤ <i>k</i> ≤ 13, -23 ≤ <i>l</i> ≤ 27	-23 ≤ <i>h</i> ≤ 23, -13 ≤ <i>k</i> ≤ 15, -20 ≤ <i>l</i> ≤ 20
Reflections collected / unique	36848 / 5033 [R _{int} = 0.0759]	12678 / 6982 [R _{int} = 0.0473]
Completeness to Θ	99.3%	99.1%
Absorption correction	multi-scan ABSCOR	multi-scan ABSCOR
Min. and max transmission	0.430 and 1.000	0.449 and 1.000
Data / restraints / parameters	5033 / 0 / 328	6982 / 2 / 517
Goodness-of-fit on F ²	1.058	1.000
Final R indices [I > 2σ(I)]	R ₁ = 0.0478, wR ₂ = 0.1212	R ₁ = 0.0485, wR ₂ = 0.1222
R indices (all data)	R ₁ = 0.0515, wR ₂ = 0.1258	R ₁ = 0.0493, wR ₂ = 0.1236
Largest diff. peak and hole (e·Å ⁻³)	1.291 and -1.788	0.696 and -0.836

[‡]Refinement method was full-matrix least-squares on F²; wavelength = 0.71073 Å. R₁ = $\sum ||F_o|| - |F_c|| / \sum |F_o||$;
wR₂ = $\{\sum [w(F_o^2 - F_c^2)^2] / \sum [w(F_o^2)^2]\}^{1/2}$.